Available online at www.sciencedirect.com
SCIENCE DIRECT
Journal of Organometallic Chemistry 691 (2006) 475–484
Journal of Organometallic Chemistry
www.elsevier.com/locate/jorganchem

Relationships between ^{57}Fe NMR, Mössbauer parameters, electrochemical properties and the structures of ferrocenylketimines

Concepción López [a,*], Ramon Bosque [a], Sonia Pérez [a], Anna Roig [b], Elies Molins [b], Xavier Solans [c], Mercè Font-Bardía [c]

[a] Departament de Química Inorgánica, Facultat de Química, Universitat de Barcelona, Martí i Franquès 1-11, E-08028-Barcelona, Spain
[b] Institut de Ciència de Materials de Barcelona (ICMAB-CSIC), Campus de la Universitat Autònoma de Barcelona, E-08193-Bellaterra, Spain
[c] Departament de Cristal·lografia, Mineralogía i Dipòsits Minerals, Facultat de Geologia, Universitat de Barcelona, Martí i Franquès s/n, E-08028-Barcelona, Spain

Received 4 July 2005; received in revised form 8 September 2005; accepted 8 September 2005
Available online 20 October 2005

Abstract

A comparative study of the electrochemical properties, ^{57}Fe NMR and Mössbauer spectroscopic data of compounds $[(\eta^5\text{-}C_5H_5)Fe\{(\eta^5\text{-}C_5H_4)\text{–}C(R^1)\text{=}N\text{–}R^2\}]$ {$R^1 = H$, $R^2 = CH_2\text{–}CH_2OH$ (**1a**), CH(Me)–CH_2OH (**1b**), $CH_2C_6H_5$ (**1c**), C_6H_4–2Me (**1d**), C_6H_4–2SMe (**1e**) or C_6H_4–2OH (**1f**) and $R^1 = C_6H_5$, $R^2 = C_6H_4$–2Me (**2d**)} is reported. The X-ray crystal structure of $[(\eta^5\text{-}C_5H_5)Fe\{(\eta^5\text{-}C_5H_4)\text{–}CH\text{=}N\text{–}C_6H_4\text{–}2OH\}]$ (**1f**) is also described. Density functional theoretical (DFT) studies of these systems have allowed us to examine the effects induced by the substituents of the "–$C(R^1)$=N–R^2" moiety or the aryl rings (in **1d–1f**) upon the electronic environment of the iron(II) centre.

Keywords: ^{57}Fe NMR; Ferrocenyl Schiff bases; Mössbauer spectra; Electrochemical properties; DFT calculations

1. Introduction

Recently, great interest has been generated in the synthesis and study of ferrocene derivatives containing one or more heteroatoms with good donor abilities, since these derivatives or their transition metal complexes have potential applications in several areas [1,2]. However, while ^{57}Fe NMR spectroscopy has been used to examine a variety of iron(II) compounds [3–6], its application to ferrocene derivatives is less common [6–10]. Most papers refer to $[(\eta^5\text{-}C_5Me_5)Fe(\eta^5\text{-}C_5Me_5)]$, ferrocenophanes and simple mono-substituted ferrocene derivatives of the type $[(\eta^5\text{-}C_5H_5)Fe(\eta^5\text{-}C_5H_4R)]$ {with R = Cl, Br, I, CN, Et, CH_2OH, CHO, C(O)Me, CO(Bu), CH(OH)Me, $C(O)C_6H_5$, $CH(OH)C_6H_5$, CO_2Me, C≡CH, $SiCl_3$, $SiMe_3$, $SiMe_2Cl$ or $SnMe_3$} [7,8] as shown in Fig. 1(a). A few articles on ^{57}Fe NMR spectra of 1,1′-disubstituted derivatives [8c,8d] have also been published and, recently, such studies have also been extended to ferrocenylamines of general formula: $[(\eta^5\text{-}C_5H_5)Fe\{(\eta^5\text{-}C_5H_4)\text{–}N(R^1)(R^2)\}]$ (Fig. 1(b)) [9].

In the last decade a wide range of ferrocenyl Schiff bases of the type $[(\eta^5\text{-}C_5H_5)Fe\{(\eta^5\text{-}C_5H_4)\text{–}C(R^1)\text{=}N\text{–}R^2\}]$ {with R^1 = H, Me, C_6H_5 and R^2 = alkylic or arylic groups} have been described and some of these bases have also been characterised by X-ray diffraction [11–14]. These compounds are stable and highly soluble in the common solvents used for NMR experiments and so they are especially attractive for ^{57}Fe NMR studies. However, to our knowledge, no such study has been reported to date. To assess the relative influence of the electronic and steric properties of the substituents (R^1 and R^2) [15] in compounds $[(\eta^5\text{-}C_5H_5)Fe\{(\eta^5\text{-}C_5H_4)\text{–}C(R^1)\text{=}N\text{–}R^2\}]$ upon the electronic environment of the iron(II) we investigated the ^{57}Fe NMR spectra of the ferrocenyl-aldimines $[(\eta^5\text{-}C_5H_5)Fe\{(\eta^5\text{-}C_5H_4)\text{–}C(H)\text{=}N\text{–}R^2\}]$ {with $R^2 = CH_2CH_2OH$ (**1a**), CH(Me)–CH_2OH

* Corresponding author.
E-mail address: conchi.lopez@qi.ub.es (C. López).

0022-328X/$ - see front matter © 2005 Elsevier B.V. All rights reserved.
doi:10.1016/j.jorganchem.2005.09.020

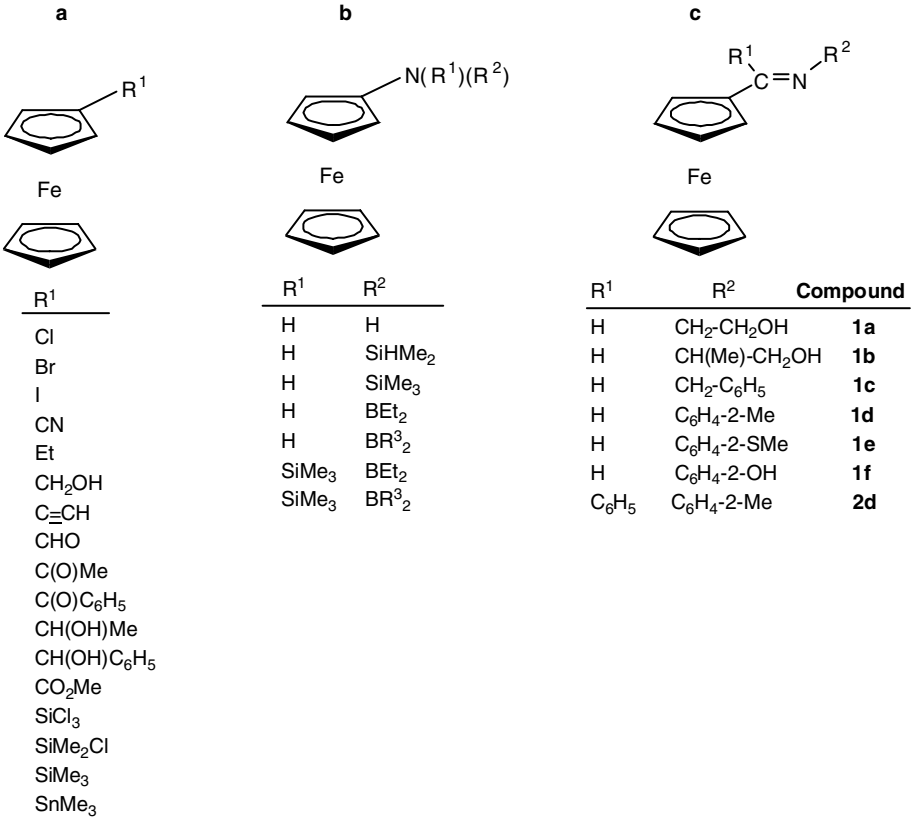

Fig. 1. Schematic view of the mono-substituted ferrocene derivatives studied by ^{57}Fe NMR spectroscopy (a and b) and the ferrocenyl Schiff bases under study (c). (The R^3 group represents: 9-borabicyclo[3.3.1]nonyl).

(**1b**), $CH_2C_6H_5$ (**1c**), C_6H_4–2Me (**1d**), C_6H_4–2SMe (**1e**) and C_6H_4–2OH (**1f**)} (Fig. 1(c)). We also attempted to correlate the ^{57}Fe chemical shifts with other properties of these compounds (such as the quadrupolar splitting value obtained from Mössbauer spectroscopy or their propensity to oxidise). Comparison of data for **1a–1f** may reveal the influence of the nature of the R^2 on the imine nitrogen and the effect of the electronic and steric properties [15] of the substituent on the *ortho* site of the aryl rings (Me, SMe or OH) in compounds **1d–1f** upon the electronic environment of the iron. The extension of these studies to complex **2d** may also clarify the effects of a hydrogen (in **1d**) or a phenyl (**2d**) in the imine carbon.

2. Results and discussion

The ferrocenyl Schiff bases: [(η^5-C_5H_5)Fe{(η^5-C_5H_4)–C(R^1)=N–R^2}] {with $R^1 = H$ and $R^2 = CH_2CH_2OH$ (**1a**), CH_2–C_6H_5 (**1c**), (S_C)-CH(Me)–CH_2OH (**1b**), C_6H_4–2Me (**1d**) or C_6H_4–2SMe (**1e**) or $R^1 = C_6H_5$ and $R^2 = C_6H_4$–2Me (**2d**)} (Fig. 1(c)) were prepared as described previously [11–14]. In addition, [(η^5-C_5H_5)Fe{(η^5-C_5H_4)–CH=N–C_6H_4–2OH}] (**1f**) was obtained using the general procedure described before for the synthesis of ferrocenyl Schiff bases of general formula [(η^5-C_5H_5)Fe{(η^5-C_5H_4)–CH=N–R^2}], where R^2 represents a phenyl, benzyl or naphthyl group [11,12,16]. This procedure consists of the reaction of equimolar amounts of ferrocenecarboxaldehyde and the corresponding amine H_2N–R^2 in refluxing benzene. A Dean-Stark apparatus was used to remove the benzene–water azeotrope formed during the reaction. For the preparation of **1f**, 2-amino-phenol was used and the reaction yielded deep red crystals suitable for X-ray diffraction. Compound **1f** was characterised by elemental analyses, FAB$^+$mass spectra and infrared spectroscopy as well as mono- and two-dimensional {NOESY, COSY, HSQC and HMBC} NMR spectroscopy and by X-ray diffraction.

The elemental analyses (see Section 3) were consistent with those expected for [(η^5-C_5H_5)Fe{(η^5-C_5H_4)–C(H)=N–(C_6H_4–2OH)}] (**1f**). The most outstanding feature of the infrared spectrum of **1f** is the presence of three absorption bands in the range 1550–1650 cm^{-1}. The band at highest wavenumber was assigned to the stretching of the >C=N– functional group [11–14,16], and the other two were attributed to the stretching of the >C=C< moieties of the aromatic phenyl group. Proton and ^{13}C{^{1}H} NMR spectroscopic data for **1f** are presented in Section 3. Signals were assigned using mono- and two-dimensional {HSQC and HMBC} NMR experiments. The {^{1}H–^{1}H} NOESY spectrum showed cross-peaks between the signals due to the imine proton and that of the H$^{6'}$ proton. This indicates that the ferrocenyl Schiff base adopts the *anti*-(*E*) conformation in solution.

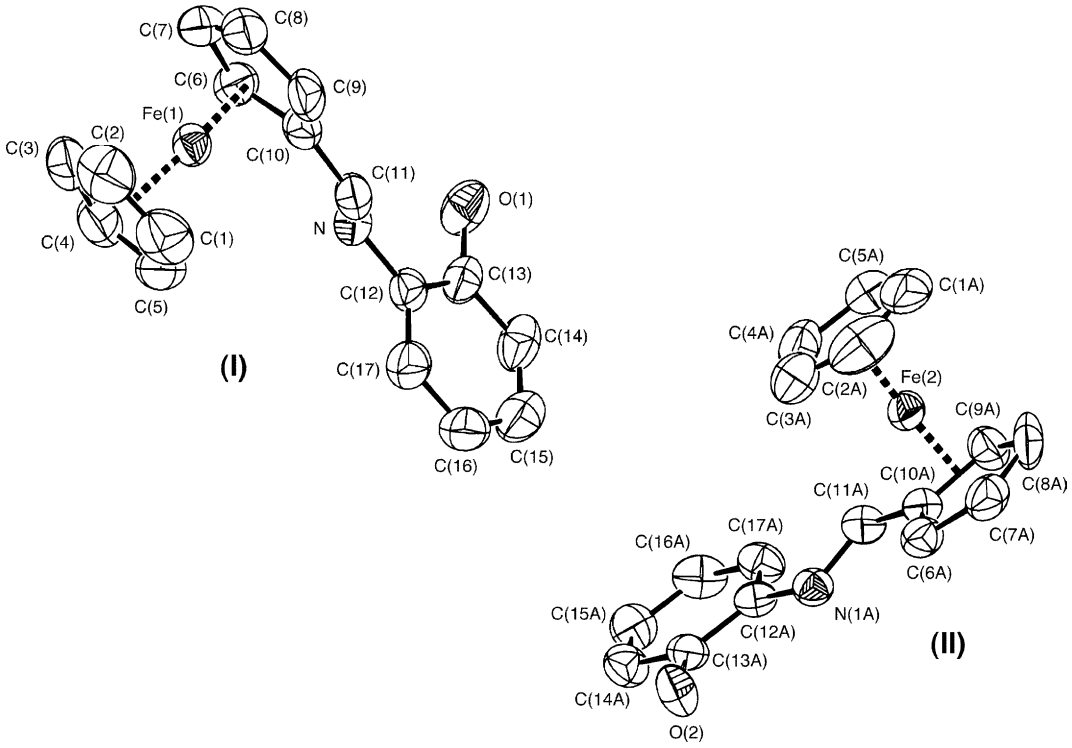

Fig. 2. Molecular structure and atom labelling scheme for the two non-equivalent molecules (**I** and **II**) found in the crystal structure of [(η^5-C_5H_5)Fe{(η^5-C_5H_4)–C(H)=N–(C_6H_4–2OH)}] (**1f**).

The remaining compounds (**1a**, **1c–1e** and **2d**) were characterised by ^{1}H NMR spectroscopy, and in all cases the number of signals as well as their multiplicities agreed with the results reported in the literature [11–13].

The two non-equivalent molecules of [(η^5-C_5H_5)Fe{(η^5-C_5H)–CH=N–(C_6H_4–2OH)}] (hereafter referred to as **I** and **II**) present in the unit cell of **1f** together with the atom labelling scheme are depicted in Fig. 2 and a selection of bond lengths and angles is presented in Table 1.

Table 1
Selected bond lengths (in Å), bond angles (in °) of [(η^5-C_5H_5)Fe{(η^5-C_5H_4)–CH=N–(C_6H_4–2OH)}] (**1f**)

Molecule **I**		Molecule **II**	
Selected bond lengths			
C(10)–C(11)	1.457(7)	C(10A)–C(11A)	1.446(7)
C(11)–N(1)	1.247(6)	C(11A)–N(1A)	1.274(6)
N(1)–C(12)	1.425(6)	N(1A)–C(12A)	1.425(5)
C(12)–C(13)	1.372(7)	C(12A)–C(13A)	1.394(6)
C(13)–O(1)	1.359(6)	C(13A)–O(2)	1.365(5)
C(13)–C(14)	1.383(7)	C(13A)–C(14A)	1.376(6)
C(14)–C(15)	1.368(9)	C(14A)–C(15A)	1.395(8)
C(15)–C(16)	1.370(9)	C(15A)–C(16A)	1.351(7)
C(16)–C(17)	1.394(8)	C(16A)–C(17A)	1.391(7)
Fe–C[a]	2.029(9)	Fe–C[a]	2.029(8)
C–C[a]	1.40(2)	C–C[a]	1.41(2)
Selected bond angles			
C(10)–C(11)–N(1)	125.5(5)	C(10A)–C(11A)–N(1A)	123.7(5)
C(11)–N(1)–C(12)	118.0(4)	C(11A)–N(1A)–C(12A)	120.3(4)
N(1)–C(12)–C(13)	119.1(5)	N(1A)–C(12A)–C(13A)	116.3(4)
N(1)–C(12)–C(17)	121.4(5)	N(1A)–C(12A)–C(17A)	125.6(4)
C(12)–C(13)–O(1)	121.6(4)	C(12A)–C(13A)–O(2)	116.6(4)
O(1)–C(13)–C(14)	118.3(5)	O(2)–C(13A)–C(14A)	122.0(4)

Standard deviations are given in parentheses.
[a] Average value for the ferrocenyl moiety.

The >C=N– bond lengths [1.247(6) Å in **I** and 1.274(6) Å in **II**] are consistent with the values reported for related ferrocenyl Schiff bases of general formula: [(η^5-C_5H_5)Fe{(η^5-C_5H_4)–C(R^1)=N–R^2}], with R^1 = H, Me or C_6H_5 [11–14,16]. The values of the torsion angles: C(10)–C(11)–N(1)–C(12) (179.2°) and C(10A)–C(11A)–N(1A)–C(12A) (178.2°) indicate that the imine adopts the *anti*-(*E*) form in the two molecules in good agreement with the results obtained for most Schiff bases derived from ferrocene [17].

Bond lengths and angles of the ferrocenyl moiety agree with those reported for most ferrocene derivatives [16]. In the two molecules the pentagonal rings are planar[1] [18,19], nearly parallel (*tilt angles*: −2.69° and

[1] In molecule **I**, the least-squares equations of the planes defined by the set of atoms [C(1)–C(5)] and [C(6)–C(10)] are: (0.7109)XO + (0.2410)YO + (0.6670)ZO = 0.8948 and (0.7426)XO + (0.2373)YO + (0.6262)ZO = 4.6278, respectively. Deviations from the plane: C(1), 0.004; C(2), −0.014; C(3), 0.019; C(4), −0.016; C(5), 0.008; C(6), −0.001; C(7), −0.002; C(8), 0.004; C(9), −0.004 and C(10), 0.003 Å. In molecule **II**, the least-squares equations of the planes defined by the set of atoms [C(1A)–C(5A)] and [C(6A)–C(10A)] are: (0.3711)XO + (0.7103)YO + (−0.5982)ZO = 3.1708 and (0.3479)XO + (0.6769)YO + (−0.6487)ZO = −0.6159, respectively. Deviations from the plane: C(1A), 0.002; C(2A), −0.003; C(3A), 0.003; C(4A), −0.002; C(5A), 0.000; C(6A), 0.006; C(7A), −0.006; C(8A), 0.004; C(9A), −0.001 and C(10A), −0.003 Å.

Table 2
Selected structural data for compounds $[(\eta^5\text{-}C_5H_5)Fe\{(\eta^5\text{-}C_5H_4)\text{–}C(R^1)\text{=}N\text{–}R^2\}]$ with $R^1 = H$, $R^2 = CH_2CH_2OH$ (**1a**), $CH_2\text{–}C_6H_5$ (**1c**), C_6H_4–2SMe (**1e**), C_6H_4–2OH (**1f**) or $R^1 = C_6H_5$ and $R^2 = C_6H_4$–2Me (**2d**)

Compound	**1a**[a]	**1c**[b]	**1e**[c,d]	**1f**[d]	**2d**[e]
N–C(11)	1.252(5) Å	1.262(7) Å	1.268(4) Å	1.260(6) Å	1.294(13) Å
C(11)–C(10)	1.459(6) Å	1.464(7) Å	1.453(2) Å	1.451(7) Å	1.44(2) Å
Fe–C[f]	2.017(5) Å	2.035(6) Å	2.04(10) Å	2.029(9) Å	2.029(15) Å
C(11)–N–C(12)	117.6(4)°	116.8(5)°	118.2(3)°	119(2)°	125.4(10)°
C(10)–C(11)–N–C(12)	173.8(5)°	178.6(6)°	179.1(4)°	179.2(4)°	176.2(16)°
Tilt angle	0.59°	1.9(6)°	1.3°	3.2°	2.7°
Twist angle	−3.4(6)°	4.3(1) °	5.1(4)°	1(1)°	2(2)°

Numbering of the atoms corresponds to the schemes shown below.

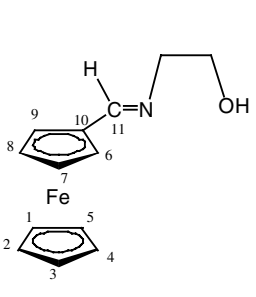

(1a)

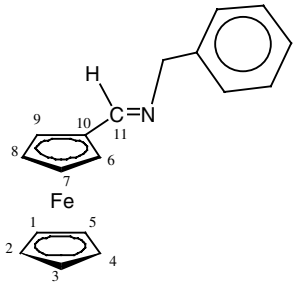

(1c)

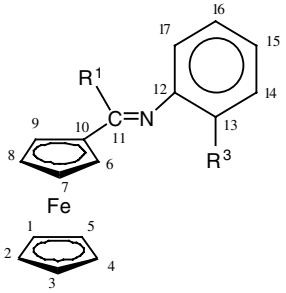

$R^1 = H$, R^3= SMe (**1e**), OH (**1f**)
R^1 = Ph, R^3 = Me (**2d**)

[a] Data from [11c].
[b] Data from [11d].
[c] Data from [12].
[d] Average values for the two non-equivalent molecules found in the crystal structures.
[e] Data from [13c].
[f] Average value for the ferrocenyl unit.

3.72° for **I** and **II,** respectively) and they deviate by ca. −0.65° (in **I**) or 2.67° (in **II**) from the ideal eclipsed conformation.

The phenyl rings are planar[2] [20] and their main planes form angles of 54.5° (in **I**) and 17.6° (in **II**) with the imine moiety.

In the crystal two neighbouring molecules of the same type (**I** or **II**) are linked by hydrogen bonds between –OH moiety and the nitrogen of a proximal molecule[3] [21]. These dimers are also connected by C–H···π interactions [18].

To sum up, data presented in Table 2 reveal that the structural parameters obtained for **1f** do not differ substantially from those obtained for the ketimines **1a**, **1c**, **1e** and **2d**. However, comparison of the X-ray crystal structures of **1e** and **1f** shows that the nature of the substituent in the *ortho* site of the phenyl ring influences the type of intermolecular interactions: C–H···S and C–H···π (in **1e**) or O–H···N and C–H···π (in **1f**). This, in turn, affects the assembly of structural units: dimers (in **1f**) or tetramers (in **1e**).

In order to ascertain the influence of the substituents on the electronic environment of the iron(II), ^{57}Fe Mössbauer studies were performed. In all cases the spectra consisted of a single quadrupole doublet (Fig. 3), thus indicating a single iron site. The isomer shift, quadrupole splitting parameters and line-widths are presented in Table 3. In ferrocene derivatives electron-donating groups increase the quadrupole splitting (ΔE_q) relative to that of ferrocene, whereas electron-pulling groups produce a decrease of the ΔE_q parameter [19]. For all the ferrocenyl-aldimines (**1a–1f**), the quadrupole splitting was smaller than that of ferrocene [20] ($\Delta E_q = 2.37$ mm s^{-1} at room temperature or 2.41 mm s^{-1} at 80 K), thus indicating that the ≥C=N– is a stronger electron-withdrawing group than the hydrogen in ferrocene. Moreover, the electron-pulling ability of the —CH=N—R^2 moieties was dependent on the nature of the R^2 fragment and increased according to the sequence: $CH(Me)\text{–}CH_2OH \leqslant CH_2C_6H_5 < CH_2CH_2OH < C_6H_4\text{–}2Me \leqslant C_6H_4\text{–}2SMe < C_6H_4\text{–}2OH$.

On the other hand, it is also well known that the study of the electrochemical properties of ferrocene derivatives provides useful information about the effect induced by the substituents on the proclivity of the iron(II) to oxidise [21]. In

[2] The least-squares equations of the planes defined by the set of atoms [C(12)-C-(17)] (in molecule **I**) and [C(12A)–C(17A)] (in molecule **II**) are: $(-0.1112)XO + (0.7414)YO + (0.6618)ZO = -1.5728$ and $(0.3384)XO + (0.7758)YO + (-0.5326)ZO = -0.1487$, respectively. Deviations from the planes: C(12), 0.008; C(13), −0.010; C(14), 0.001; C(15), 0.010; C(16), −0.012; C(17), 0.003; C(12A), 0.011; C(13A), −0.010; C(14A), 0.002; C(15A), 0.003; C(16A), −0.001 and C(17A), −0.006 Å.
[3] Donor–acceptor separation O···N = 2.845(7) Å (in **I**) and 2.929(7) Å (in **II**).

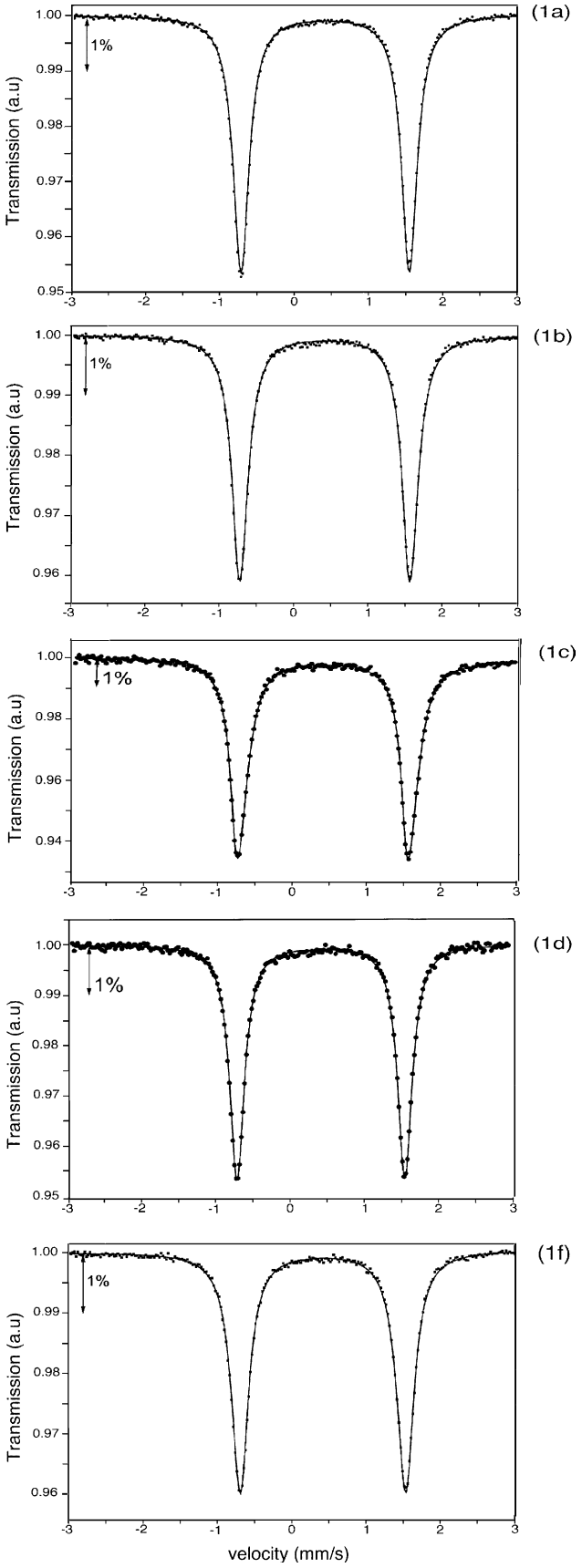

Fig. 3. Mössbauer spectra (at 80 K) of compounds: [(η^5-C_5H_5)Fe{(η^5-C_5H_4)–C(H)=N–R^2}] with R^2 = CH_2CH_2OH (**1a**), CH(Me)CH_2OH (**1b**), CH_2–C_6H_5(**1c**), C_6H_4–2Me (**1d**) and C_6H_4–2OH (**1f**).

view of this and in order to gain further insight into the effects induced by the substituents (R^1 and R^2) of the ferrocenyl Schiff bases upon their electrochemical properties, cyclic voltammetric studies were carried out. Cyclic voltammograms for **1b–1d** and **1e** are presented in Fig. 4 and the most relevant electrochemical data are summarised in Table 3.

Except for **1a**, the cyclic voltammograms exhibited an anodic peak with a directly associated reduction in the reverse scan. For **1b–1d** and **1e** the separation between peaks (ΔE) departs appreciably from the value of 59 mV (theoretically expected for an electrochemical reversible one-electron step oxidation–reduction process [22]), suggesting that a structural reorganisation takes place on oxidation. It is widely accepted that oxidation involves the loss of one electron located on the highest occupied molecular orbital (HOMO), and the results obtained from the theoretical studies described below indicate that the HOMO is not solely iron based. For **1a**, the presence of the peak due to the reduction process could not be clearly identified under these experimental conditions.

Previous electrochemical studies on mono-substituted ferrocene derivatives have demonstrated that the presence of electron donor groups increase the proclivity of the ferrocenyl unit to oxidise, which is reflected in a shift of the anodic peak to more cathodic potentials. On the other hand, for derivatives holding electron-withdrawing groups the trend is the opposite [21]. For compounds **1a–1f**, the anodic peaks appeared at higher potentials than for ferrocene, thus suggesting that the –C(H)=N–R^2 groups have a greater electron-withdrawing ability than the hydrogen in ferrocene. Moreover, comparison of data presented in Table 3 indicate that the E_{pa} values are also dependent on the nature of the R^2 group and increase according to the sequence: $CH_2CH_2OH \approx$ CH(Me)–$CH_2OH \leqslant CH_2C_6H_5 <$ C_6H_4–2Me < C_6H_4–2SMe < C_6H_4–2OH. These findings suggest that the replacement of the Me group in [(η^5-C_5H_5)Fe{(η^5-C_5H_4)–CH=N–(C_6H_4–2Me)}] (**1d**) by a SMe (in **1e**) or a OH (in **1f**) hinders the oxidation of the ferrocenyl moiety. Although these changes take place further away from the "(η^5-C_5H_5)Fe(η^5-C_5H_4)" fragment than in **1a** or **1b**, they appear to influence the electronic environment of the Fe(II), modifying the proclivity of the ferrocenyl unit to oxidise and the quadupolar splitting parameters obtained from Mössbauer spectroscopy.

Previous studies on ^{57}Fe NMR spectroscopy of the mono-substituted derivatives: [(η^5-C_5H_5)Fe(η^5-C_5H_4R)] shown in Fig. 1(b) have revealed that the presence of electron-pulling R groups produces a decrease of the electronic density of the iron (II) which is commonly associated with a downfield shift of the signal [8]. Compounds **1a–1f** were also characterised in solution by ^{57}Fe NMR spectroscopy and the chemical shifts are presented in Table 3.

Since the chemical shifts obtained for all the compounds under study are greater than that of ferrocene [δ^{57}Fe = 1535 ppm under identical experimental conditions], these findings confirm the electron-withdrawing nature of the "–CH=N–R^2" moieties in good agreement with the results

Table 3
Iron-57 Mössbauer hyperfine parameters (at 80 K) [isomer shift (i.s.), quadrupole splitting (ΔE_q) and full-width at half-height (in mm s^{-1}) (standard deviation parameters are given in parentheses)], summary of electrochemical data [anodic (E_{pa}) and cathodic potentials (E_{pa}), half-wave potentials, $E_{1/2}$(Fc), separation of the peaks for the samples (ΔE) and the intensity ratio: I_{pa}/I_{pc}, all these values were obtained using a scan rate $\upsilon = 100$ mV s^{-1} and the potentials are given in mV] and ^{57}Fe NMR-chemical shifts (in ppm) for the ferrocenylimines [(η^5-C_5H_5)Fe(η^5-C_5H_4)–C(R^1)=N–R^2}] (**1a–1f**)

Compound	R^1	R^2	Mössbauer hyperfine parameters			Electrochemical data					^{57}Fe NMR data
			i.s.	ΔEq	Γ	E_{pa}	E_{pc}	$E_{1/2}$(Fc)	ΔE	I_{pa}/I_{pc}	δ(^{57}Fe)
1a	H	CH_2–CH_2OH	0.528(1)	2.260(1)	0.256(2)	192	[a]	[a]	144	[a]	1720.6
1b	H	CH(Me)CH_2OH	0.529(1)	2.280(1)	0.258(2)	195	58	126	135	1.30	1721.5
1c	H	CH_2–C_6H_5	0.523(1)	2.277(2)	0.271(2)	202	98	150	104	1.4	1722.3
1d	H	C_6H_4–2-Me	0.525(2)	2.255(4)	0.237(4)	232	157	194	75	1.05	1754.4
1e	H	C_6H_4–2-SMe[b]	0.502(5)	2.251(4)	0.36(1)	250	191	184	132	[c]	1771.7
1f	H	C_6H_4–2-OH	0.527(1)	2.219(1)	0.278(2)	258	178	218	80	1.82	1789.9

[a] In this case the position of the cathodic peak in the reverse scan could not be clearly detected.
[b] Data from [12].
[c] Data not given.

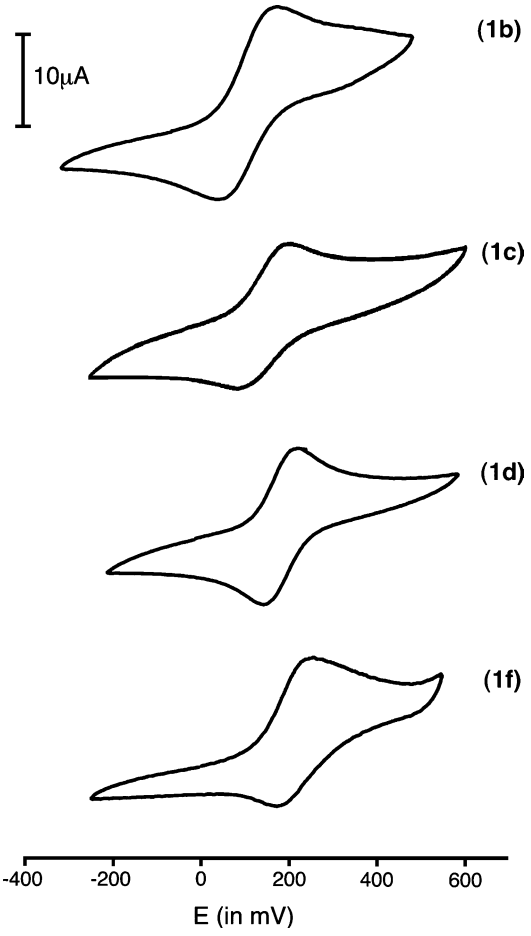

Fig. 4. Cyclic voltammograms of compounds [(η^5-C_5H_5)Fe{(η^5-C_5H_4)–C(H)=N–R^2}] with R^2 = CH(Me)CH_2OH (**1b**), CH_2–C_6H_5(**1c**), C_6H_4–2Me (**1d**) and C_6H_4–2OH (**1f**).

obtained from Mössbauer spectroscopy and the electrochemical studies described in the previous paragraphs. Additionally, comparison of the data shown in Table 3 indicates that the ^{57}Fe-chemical shifts increase according to the sequence: **1a** ⩽ **1b** ⩽ **1c** < **1d** < **1e** < **1f**. This trend is very similar to that obtained from the electrochemical studies. Moreover, in this case, tiny changes in the nature of the group bound in the *ortho* site of the phenyl ring also appear to induce greater modifications in the environment of the iron than when the substitution takes place on the alkylic chain of **1a** and **1b**. In addition, for **1d** and **2d**, which differ in the nature of the R^1 group on the imine carbon, the replacement of the H (in **1d**) by the phenyl (in **2d**)[4] produces a downfield shift of the signal of ca. 35 ppm, indicating a greater electron-withdrawing character of the "–C(C_6H_5)=N–(C_6H_4–2Me)" fragment when compared with that of the "–CH=N–(C_6H_4–2Me)".

As a first attempt to explain why for **1d–1f** the properties of the iron(II) appear to be more sensitive to the substituent effects than for compounds **1a–1b**, we performed DFT calculations of the imines **1d** and **1f** and to compare the results obtained with those recently reported for complex **1e** [12]. All the calculations were carried out using the B3LYP hybrid functional [23] and the LANL2DZ basis set [24] implemented in the GAUSSIAN 98 program [25]. The geometries were optimised without imposing any restriction.

For **1f**, bond lengths and angles obtained for the optimised geometry were consistent with those obtained from the crystallographic studies (the differences do not clearly exceed 3σ). However, in the optimised geometry the phenyl ring and the OH group were nearly co-planar with the imine moiety. This finding differs from the results obtained from the X-ray crystal structure, which showed that two neighbouring molecules were assembled in the crystal forming a dimeric unit. It should be noted that the procedure used to optimise the geometry of **1d** and **1f** does not takes intermolecular contacts into account.

As shown in Figs. 5(a)–(d), the HOMO and LUMO orbitals for **1d** and **1f** are not solely iron based. Moreover, the comparison of the HOMO orbitals for **1d** and **1f** reveals that the replacement of the Me (in **1d**) by a OH group (in **1f**) produces a considerable increase of the contributions of: (a) the $2p_z$ atomic orbital of the imine carbon and (b) the non-bonding π orbital of the aryl ring. For **1f** the $2p_z$ atomic orbital of the oxygen is also involved in the HOMO.

[4] For **2d**: δ(^{57}Fe) = 1789.9 ppm under identical experimental conditions.

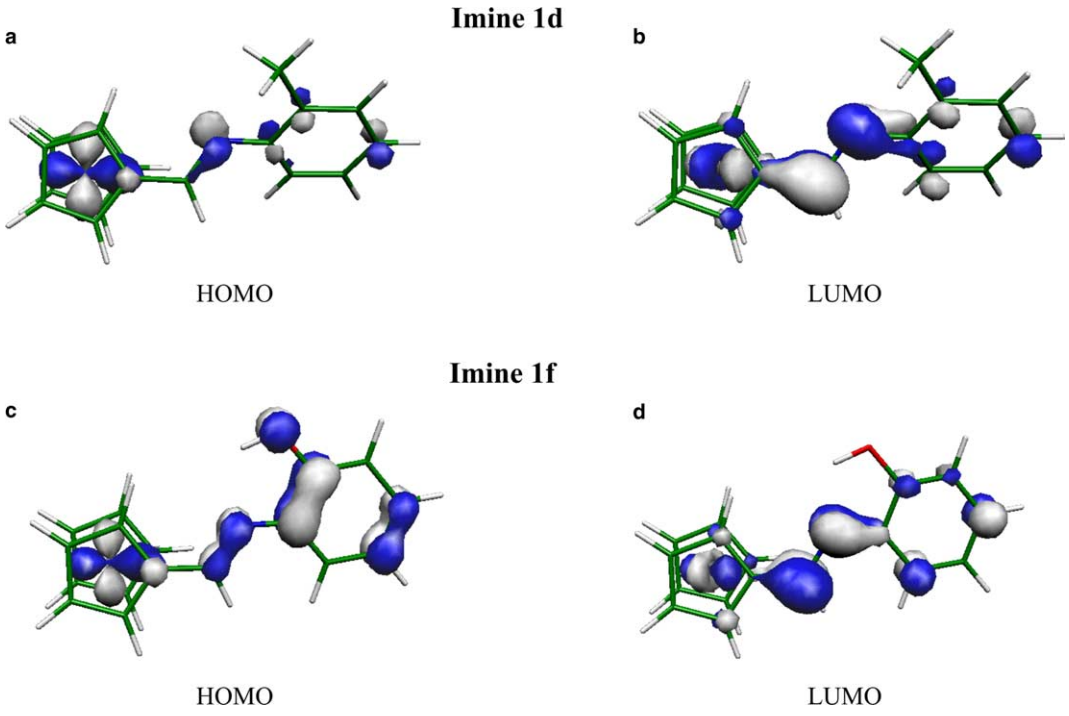

Fig. 5. HOMO and LUMO for the imines **1d** (a and b) and **1f** (c and d).

As a consequence of these findings the degree of the contribution of the atomic orbital of the iron is greater in **1d** (0.28) than in **1f** (0.20). The LUMO orbitals of **1d** and **1f** (Fig. 5(b) and (d)) are similar and the contribution of the atomic orbitals of the iron does not differ significantly.

On the other hand, the values of the Mulliken charges on the Fe(II) for the three complexes [−0.1556 (for **1d**), −0.1546 (for **1e**) and −0.1537 (for **1f**)] increase according to the sequence **1d** < **1e** < **1f**.

Recently, some authors have reported that the ^{57}Fe shielding and the chemical shifts of ferrocene and $Fe(CO)_5$ are determined by the d–d occupied-virtual couplings, and the magnitude of this coupling is inversely proportional to the energy difference between the orbitals involved [10], and the stronger deshielding observed for ferrocene when compared with that of $[Fe(CO)_5]$ was rationalised on the basis of the smaller HOMO–LUMO gap in ferrocene {2.77 eV versus 3.72 eV in $[Fe(CO)_5]$} [4,10]. For **1d–1f**, the HOMO–LUMO gap decreases according to the sequence: **1d** (4.11 eV) > **1e** (3.86 eV) > **1f** (3.79 eV). As expected, this follows the opposite trend observed for the ^{57}Fe-chemical shifts (Table 3).

3. Experimental

3.1. Materials and methods

The ferrocenyl-aldimines: $[(\eta^5\text{-}C_5H_5)Fe\{(\eta^5\text{-}C_5H_4)\text{–}CH{=}N\text{–}R^2\}]$ {with $R^2 = CH_2CH_2OH$ (**1a**), (S_C)-CH(Me)-CH_2OH (**1b**), $CH_2\text{–}C_6H_5$ (**1c**), C_6H_4–2Me (**1d**) and C_6H_4–2-SMe (**1e**)} and $[(\eta^5\text{-}C_5H_5)Fe\{(\eta^5\text{-}C_5H_4)\text{–}C(C_6H_5){=}N\text{–}(C_6H_4\text{–}2Me)\}]$ (**2d**) were prepared as described previously [11–14]. The preparations described below require the use of *highly hazardous materials*, as benzene, which should be handled with *caution*!

Elemental analyses (C, H and N) were carried out at the *Serveis de Recursos Cientifics i Tècnics* (Universitat Rovira i Virgili, Tarragona). FAB^+ mass spectra were performed at the *Servei d'Espectrometria de Masses* (Universitat de Barcelona) using 3-nitrobenzylalcohol (NBA) as matrix. Infrared spectra were obtained with a Nicolet 400-FTIR instrument using KBr pellets. Routine ^{1}H NMR spectra and $^{13}C\{^1H\}$ NMR spectra were obtained with a Gemini-200 MHz and a Bruker 250-DXR. High resolution ^{1}H NMR spectra and the two-dimensional [$\{^1H\text{–}^1H\}$ NOESY and COSY or $\{^1H\text{–}^{13}C\}$-heteronuclear single quantum coherence (HSQC) and heteronuclear multiple bond coherence (HMBC)] NMR experiments were recorded with either a Varian VRX-500 or a Bruker Advance DMX-500 instrument at 20 °C. In all cases the solvent used for the ^{1}H and $^{13}C\{^1H\}$ NMR as well as for the two-dimensional NMR experiments was $CDCl_3$ (99.8%) and $SiMe_4$ was used as internal reference. The chemical shifts (δ) are given in ppm and the coupling constants (J) in Hz.

3.2. Preparation of $[(\eta^5\text{-}C_5H_5)Fe\{(\eta^5\text{-}C_5H_4)\text{–}CH{=}N\text{–}C_6H_4\text{–}2OH\}]$ (**1f**)

A suspension formed by ferrocenecarboxaldehyde (1.024 g, 4.78×10^{-3} mol) and 50 mL of benzene was stirred at room temperature (ca. 20 °C) for 20 min and filtered

out. Then the stoichiometric amount of H_2N–(C_6H_4–2OH) was added to the filtrate. The reaction flask was connected to a condenser equipped with a Dean-Stark apparatus. The mixture was refluxed until ca. 15 mL of the benzene–water azeotrope had condensed on the Dean-Stark apparatus. The hot solution was filtered out and concentrated to ca. 5 mL. Slow evaporation of the solvent at room temperature (ca. 20 °C) produced deep red crystals suitable for X-ray analyses. (Yield: 1.21 g, 82%).*Characterisation data*: Anal. (%) Calc. for $C_{17}H_{15}NOFe$ (found): C, 66.91 (67.3); H, 4.95(5.0) and N, 4.59 (4.7). MS (FAB^+): m/z = 305.2, [M+]. IR (in cm^{-1}): 1619, ν(>C=N–); 1593 and 1579 ν(>C=C<). ^1H NMR-data: $\delta = 8.56$ [s, 1H, –CH=N–], 4.23 [s, 5H, C_5H_5], 4.82 [t, 2H, H^2 and H^5, $^3J = 2$], 4.53 [t, 2H, H^3 and H^4, $^3J = 2$], 6.99 [dd, 1H, $H^{3'}$, $^3J = 8.0$ and $^4J = 1.5$], 6.90 [td, 1H, $H^{4'}$, $^3J = 8.0$ and $^4J = 1.5$], 7.17 [td, 1H, $H^{5'}$, $^3J = 8.0$ and $^4J = 1.5$], 7.23 [dd, 1H, $H^{6'}$, $^3J = 8.0$ and $^4J = 1.5$] ppm and the signal due to the proton of the OH moiety was partially masked by the resonance of the $H^{6'}$ proton of the aryl ring. $^{13}C\{^1H\}$ NMR data: $\delta = 158.7$ [–CH=N], 69.5 [C_5H_5], 80.4 [C^1], 69.2 [C^2 and C^5], 71.7 [C^3 and C^4], 151.5 [$C^{1'}$], 136.6 [$C^{2'}$], 114.7 [$C^{3'}$], 120.1 [$C^{4'}$], 127.8 [$C^{5'}$] and 115.6 [$C^{6'}$] ppm.

3.3. ^{57}Fe Mössbauer spectra

Mössbauer spectra were recorded using powdered solid samples. The samples were placed in liquid N_2, quenched to 80 K and transferred to an Oxford Instrument cryostat. The spectra were collected at 80 K using a constant acceleration Mössbauer spectrometer with a $^{57}Co/Rh$ source. The source was moved via triangular velocity wave and the γ-counts were collected in a 512 multi-channel analyser. The data were folded, plotted and fitted by a computer procedure. Velocity calibration was done using a 25 μm thick metallic iron foil and the Mössbauer spectral parameters (presented in Table 3) are given relative to this standard at room temperature.

3.4. Electrochemical studies

Electrochemical data for compounds under study were obtained by cyclic voltammetry under nitrogen at 20 °C using acetonitrile HPLC grade as solvent and tetrabutylammonium hexafluorophosphate, {(Bu_4N)[PF_6]} (0.1 M) as supporting electrolyte and a potentiostat M263A from EG&G instruments. The half-wave potentials $E_{1/2}$ were referred to an Ag–$AgNO_3$ (0.1 M in acetonitrile) electrode separated from the solution by a medium porosity fritted disk. A platinum wire auxiliary electrode was used in conjunction with a platinum disc working Tacussel-Edi rotatory electrode (3.14 mm^2). Cyclic voltammograms of ferrocene were recorded before and after each sample to ensure the stability of the Ag–$AgNO_3$ electrode. Cyclic voltammograms of freshly prepared solutions (10^{-3}M) of the samples in acetonitrile were run and the average values of the potentials were then referred to ferrocene. In all the experiments, the cyclic voltammograms were registered using scan speeds varying from $\upsilon = 10$ to 100 mV s^{-1}.

3.5. ^{57}Fe NMR studies

A Bruker DRX 500 spectrometer, equipped with a low-γ triple resonance probe head (5 mm o.d. tubes with saturated solutions of the compounds in CD_2Cl_2, at 23 °C), was used for measuring the 16.2 MHz ^{57}Fe NMR spectra. The $^{57}Fe\{^1H\}$ NMR spectra were recorded with single pulse technique. 30° Pulses were applied (10 000–20 000 transients, 6–12 h of spectrometer time), and the duration of the 90° pulse was 80 μs, calibrated by determining the pulse length for the ^{73}Ge NMR signal of $GeCl_4$. ^{57}Fe chemical shifts are given relative to neat [$Fe(CO)_5$] ($\delta^{57}Fe = 0$ with $\Xi(^{57}Fe) = 3.237798$).

3.6. Crystallography

A prismatic crystal (0.1 × 0.1 × 0.2 mm) of [(η^5-C_5H_5)Fe{(η^5-C_5H_4)–CH=N–(C_6H_4–2OH)}] (**1f**) was selected and mounted on a MAR345 diffractometer with image plate detector. Unit-cell parameters were determined from automatic centring of 6447 reflections ($3° < \Theta < 31°$) and refined by full-matrix least-squares method. Intensities were collected with a graphite monochromatised Mo Kα radiation. The number of reflections measured in the range $2.00° \leqslant \Theta \leqslant 25.02°$ was 15 366, of which 8571 were non-equivalent by symmetry {R_{int}(on I) = 0.057. The number of reflections assumed as observed applying the condition $I > 2\sigma(I)$ was 2591. Lorentz-polarisation corrections were made but absorption corrections were not.

The structure was solved by Direct methods using SHELXS computer program [26] and refined by full-matrix least-squares method with the SHELX97 computer program [27] using 6447 reflections (very negative intensities were not assumed). The function minimised was $\sum w||F_o|^2 - |F_c|^2|^2$, where $w = [\sigma^2(I) + (0.0722P)^2]^{-1}$ and $P = |F_o| + 2|F_c|^2/3$ were taken from the literature [28]. Twenty-six hydrogen atoms were located from a difference synthesis and refined with an overall isotropic temperature factor. Six hydrogen atoms were computed and refined using a riding model with an isotropic temperature factor equal to 1.2 times the equivalent temperature factor of the atom to which is linked. The final R (on F) factor was 0.052, wR (on $|F|^2$) = 0.117 and other relevant parameters concerning the resolution and refinement of this crystal structure are presented in Table 4.

3.7. Theoretical studies

Calculations were carried out at the B3LYP computational level [23] with the GAUSSIAN 98 package [25] using the LANL2DZ basis set [24]. Geometry optimisations were performed without any geometry restriction.

Table 4
Crystal data and details of the refinement of the crystal structure of [(η^5-C_5H_5)Fe{(η^5-C_5H_4)–C(H)=N–(C_6H_4-2-OH)}] (**1f**)

	1f
Empirical formula	$C_{17}H_{15}FeNO$
Formula weight	305.15
Crystal size (mm × mm × mm)	0.1 × 0.1 × 0.2
Temperature (K)	293(2)
Wavelength (Å)	0.71069
Crystal system	Monoclinic
Space group	*C*2/*c*
a (Å)	25.4260(12)
b (Å)	17.7992(8)
c (Å)	15.3070(10)
$\alpha = \gamma$ (°)	90.000(2)
β (°)	126.9410(10)
Volume (Å^3)	5536.7(5)
Z	16
D_{calc} (Mg m^{-3})	1.464
Absorption coefficient (mm^{-1})	1.083
F(000)	2528
Θ range for data collection (°)	2.00–25.02
Index ranges	$-23 \leqslant h \leqslant 30$, $-20 \leqslant k \leqslant 20$ and $-17 \leqslant l \leqslant 0$
No. of reflections collected	15366
No. of unique reflections [R_{int}]	8571 [0.0570]
No. of data	6447
No. of parameters	465
Goodness of fit on F^2	0.989
Final *R* indices [$I>2\sigma(I)$]	$R_1 = 0.0522$, $wR_2 = 0.1170$
R indices (all data)	$R_1 = 0.1146$, $wR_2 = 0.1372$
Largest difference peak and hole (e Å^{-3})	0.436 and −0.533

Standard deviation parameters are given in parentheses.

4. Supplementary materials

Crystallographic data for the structural analyses of [(η^5-C_5H_5)Fe{(η^5-C_5H_4)–CH=N–(C_6H_4–2OH)}] (**1f**) have been deposited at the Cambridge Crystallographic Data Centre: CCDC No. 273566. Copies of this information can be obtained from: The Director, CCDC, 12 Union Road, Cambridge CB2 1EZ, UK (fax: +44 1233 336 033; e-mail: deposit@ccdc.ac.uk or www.ccdc.cam.ac).

Acknowledgements

We are grateful to Prof. Bernd Wrackmeyer (University of Bayreuth, Germany) for providing ^{57}Fe NMR data. This work was supported by the Ministerio de Ciencia y Tecnología of Spain, the Generalitat de Catalunya (Grants: BQU2003-00906 and 2001-SRG-00045) and FEDER funds.

References

[1] A. Togni, T. Hayashi (Eds.), Ferrocenes. Homogeneous Catalysis, Organic Synthesis and Materials Science, VCH, Weinheim, Germany, 1995.
[2] For a general overview of recent applications of these derivatives, see for instance the articles included in the special issue devoted to ferrocene derivatives published on J. Organomet. Chem. (2002) 637–639.
[3] For a review on ^{57}Fe-NMR spectroscopy see R. Benn, in: P.S. Pregosin (Ed.), Transition Metal NMR, Elsevier, Amsterdam, Netherlands, 1991, p. 103.
[4] C.H. Eisenbroich, A. Salzer, Organometallics, A Concise Introduction, VCH, Weinheim, Germany, 1989, p. 370.
[5] For recent contributions involving ^{57}Fe-NMR spectroscopy see for instance: (a) M. Buehl, F.T. Mauschick, Phys. Chem. 4 (2002) 5508; (b) M. Buehl, F.T. Mauschick, F. Terstegen, B. Wrackmeyer, Angew. Chem. Int. Ed. 41 (2002) 2312.
[6] For theoretical studies involving ^{57}Fe-NMR spectroscopy see for instance: M. Buehl, O.L. Malkina, V.G. Malkin, Helv. Chim. Acta 79 (1996) 742.
[7] B. Wrackmeyer, O.L. Tok, A. Ayazi, F. Hertel, M. Herberhold, Z. Naturforsch. (2002) 305.
[8] (a) A.A. Koridze, N.M. Astahova, P.V. Petrovskii, J. Organomet. Chem. 254 (1983) 345; (b) E. Haslinger, K. Koci, W. Robien, K. Schlogl, Monatsch. Chem. 114 (1983) 495; (c) B. Wrackmeyer, A. Azayi, H.E. Maisel, M. Herberhold, J. Organomet. Chem. 630 (2001) 263; (d) A. Houlton, J.R. Miller, R.M.G. Roberts, J. Silver, J. Chem. Soc., Dalton Trans. (1991) 467.
[9] B. Wrackmeyer, H.E. Maisel, M. Herberhold, Z. Naturforsch. (2001) 1373.
[10] For theoretical studies focused on ^{57}Fe-NMR spectroscopy of ferrocene, see: G. Schreckenback, J. Chem. Phys. 110 (1999) 11936, and references therein.
[11] (a) C. López, J. Sales, X. Solans, R. Zquiak, J. Chem. Soc., Dalton Trans. (1992) 2321; (b) R. Bosque, C. López, J. Sales, X. Solans, M. Font-Bardía, J. Chem. Soc., Dalton Trans. (1994) 735; (c) C. López, A. Caubet, X. Solans, M. Font-Bardía, J. Organomet. Chem. 598 (2000) 87; (d) R. Bosque, M. Font-Bardía, C. López, J. Sales, J. Silver, X. Solans, J. Chem. Soc., Dalton Trans. (1994) 747.
[12] S. Pérez, C. López, A. Caubet, R. Bosque, X. Solans, M. Font-Bardía, A. Roig, E. Molins, Organometallics 23 (2004) 224.
[13] (a) R. Bosque, C. López, J. Sales, X. Solans, J. Organomet. Chem. 483 (1994) 61; (b) C. López, R. Bosque, X. Solans, M. Font-Bardía, New J. Chem. 20 (1996) 1285; (c) C. López, A. Caubet, S. Pérez, X. Solans, X. Font-Bardía, Chem. Commun. (2004) 540.
[14] (a) Y.J. Wu, S.Q. Huo, Y. Zhu, J. Organomet. Chem. 485 (1995) 161; (b) J. Silver, J.R. Miller, A. Houlton, H.T. Ahmet, J. Chem. Soc., Dalton Trans. (1994) 3355; (c) A. Houlton, J.R. Miller, J. Silver, N. Jassim, T.L. Axon, D. Bloor, G.H. Gross, Inorg. Chim. Acta 205 (1995) 67; (d) T. Tsutsumi, M. Okubo, N. Kasahara, Y. Katsube, Bull. Chem. Soc. Jpn. 61 (1988) 237.
[15] C. Hansch, A. Leo, D. Koekman, Exploring QSAR. Hydrophobic Electronic and Steric Constants, ACS, Washinghton, USA, 1995.
[16] (a) M. Benito, C. López, X. Morvan, Polyhedron 18 (1999) 2583; (b) M. Benito, C. López, X. Solans, M. Font-Bardía, Tetrahedron: Asymmetry 9 (1998) 4219.
[17] T.H. Allen, O. Kennard, Chem. Des. Automat. News 8 (1993) 128.
[18] N. Nishio, M. Hirota, Y. Umezakwo, The C–H···π Interaction, Wiley-VCH, New York, USA, 1988.
[19] (a) A. Houlton, J.R. Miller, J. Silver, N. Jasim, M.T.H. Ahmet, T.L. Axon, D. Bloor, G.H. Cross, Inorg. Chim. Acta 205 (1993) 65; (b) A. Houlton, J.R. Miller, R.G.M. Roberts, J. Silver, J. Chem. Soc., Dalton Trans. (1991) 467.
[20] A. Houlton, P.T. Bishop, R.G.M. Roberts, J. Silver, M. Herberhold, J. Organomet. Chem. 346 (1989) 381.
[21] (a) G.L. Hoh, W.W. Mc Ewewn, J.J. Kleinberg, J. Am. Chem. Soc. 83 (1961) 3949;

(b) W.F. Little, C.N. Reilley, J.D. Jonson, A.P. Saunders, J. Am. Chem. Soc. 86 (1964) 1376;
(c) N.F. Blom, W.W. Neuse, H.G. Thomas, Transition Met. Chem. 12 (1987) 301;
(d) P. Zanello, A. Cinquantini, S. Mangani, G. Opromolla, L. Pardi, C. Janiak, M.D. Rausch, J. Organomet. Chem. 471 (1994) 171;
(e) A. Benito, J. Cano, R. Martínez, J. Soto, J. Payá, F. Lloret, M. Julve, J. Faus, M.D. Cano, Inorg. Chem. 32 (1993) 1197;
(f) M. Bracci, E. Ercolani, B. Floris, M. Bassetti, A. Chiessi-Vila, C. Guastini, J. Chem. Soc., Dalton Trans. (1990) 1357;
(g) A. Louati, M. Gross, L. Duce, D. Mat, J. Organomet. Chem. 463 (1993) 169.

[22] E.R. Brown, J.R. Sandifer, in: B.W. Rossiter, J.H. Hamilton (Eds.), Physical Methods in Chemistry. Electrochemical Methods, vol. 4, Wiley, New York, USA, 1986 (Chapter 4).

[23] (a) A.D. Becke, J. Chem. Phys. 98 (1993) 5648;
(b) C. Lee, W. Yang, R.G. Parr, Phys. Rev. B 37 (1988) 785.

[24] (a) P.J. Hay, W.R. Wadt, J. Chem. Phys. 82 (1985) 270;
(b) W.R. Wadt, P.J. Hay, J. Chem. Phys. 82 (1985) 284;
(c) P.J. Hay, W.R. Wadt, J. Chem. Phys. 82 (1985) 299.

[25] M.J. Frisch, G.W. Trucks, H.B. Schleger, G.E. Scuseria, M.A. Robb, J.R. Cheesemand, V.G. Zarkrzewsi, J.A. Montgomery Jr., R.E. Stratmann, J.C. Burant, S. Dapprich, J.M. Millam, A.D. Daniels, K.N. Kudin, M.C. Strain, O. Farkas, J. Tomasi, V. Barone, M. Cossi, R. Cammi, B. Menucci, C. Pomelli, C. Adamo, S. Cliffored, J. Ochterski, G.A. Peterson, P.Y. Ayala, Q. Cui, K. Morokuma, P. Salvador, J.J. Dannenberg, D.K. Malick, A.D. Rabuck, K. Raghavachari, J.B. Foresman, J. Cioslowski, J.V. Ortiz, A.G. Baboul, B.B. Stefanov, G. Liu, A. Liashenko, P. Piskorz, I. Komaromi, R. Gomperts, R.L. Martin, D.J. Fox, T. Keith, M.A. Al-Laham, C.Y. Peng, A. Nanayakkara, M. Challacombe, P.N.W. Gill, B. Johnson, W. Chen, M.W. Wong, J.L. Andres, C. González, M. Head-Gordon, E.S. Replogle, J.A. Pople, GAUSSIAN 98, revision A.11, Gaussian Inc., Pittsburg, USA, 2001.

[26] G.M. Sheldrick, SHELXS. A Computer Program for Determination of Crystal Structures, University of Göttingen, Germany, 1997.

[27] G.M. Sheldrick, SHELX97. A Computer Program for Determination of Crystal Structures, University of Göttingen, Germany, 1997.

[28] International Tables of X-ray Crystallography, vol. IV, Kynoch Press, 1974, pp. 99–100, 149.